Understanding the effects of radiative preheat and self-emission from shock heating on equation of state measurement at 100s of Mbar using spherically converging shock waves in a NIF hohlraum (F)

Joseph Nilsen,[1] (ID) Andrea L. Kritcher,[1] Madison E. Martin,[1] Robert E. Tipton,[1] Heather D. Whitley,[1] (ID)
Damian C. Swift,[1] Tilo Döppner,[1] Benjamin L. Bachmann,[1] (ID) Amy E. Lazicki,[1] Natalie B. Kostinski,[1] (ID)
Brian R. Maddox,[1] Gilbert W. Collins,[2] Siegfried H. Glenzer,[3] (ID) and Roger W. Falcone[4]

AFFILIATIONS

[1] Lawrence Livermore National Laboratory, Livermore, California 94551, USA
[2] University of Rochester, Rochester, New York 14627, USA
[3] SLAC National Accelerator, Menlo Park, California 94025, USA
[4] University of California Berkeley, Berkeley, California 94720, USA

ABSTRACT

Over the last six years many experiments have been done at the National Ignition Facility to measure the Hugoniot of materials, such as CH plastic at extreme pressures, up to 800 Mbar. The "Gbar" design employs a strong spherically converging shock launched through a solid ball of material using a hohlraum radiation drive. The shock front conditions are characterized using x-ray radiography. In this paper we examine the role of radiation in heating the unshocked material in front of the shock to understand the impact it has on equation of state measurements and how it drives the measured data off the theoretical Hugoniot curve. In particular, the two main sources of radiation heating are the preheating of the unshocked material by the high-energy kilo-electron-volt x-rays in the hohlraum and the heating of the material in front of the shock, as the shocked material becomes hot enough to radiate significantly. Using our model, we estimate that preheating can reach 4 eV in unshocked material, and that radiation heating can begin to drive data off the Hugoniot significantly, as pressures reach above 400 Mb.

I. INTRODUCTION

Laboratory measurements of matter at high energy density is of great importance in understanding the structure and evolution of astrophysical objects, such as gas-giant planets, brown dwarfs, and highly evolved stars, where extreme pressures can exceed 100 Mbar and reach well into the Gbar range.[1-3] At Lawrence Livermore National Laboratory (LLNL) the Gbar experimental platform has been developed and demonstrated[4-6] to study the shock compression (Hugoniot) of material compressed to near Gbar pressures, in a spherically converging geometry, using streaked x-ray radiography. In these experiments, the National Ignition Facility (NIF) laser heats the inside of a gold hohlraum and creates an x-ray radiation drive

which ablates an outer ablator, sending a strong spherical shock into a solid sphere of material. The shock velocity and density spike at the shock front are characterized using x-ray radiography to determine the pressure and density along the shock Hugoniot, as the shock travels to the center of the solid sphere. As the shock travels towards the center, pressure increases as ~1/radius, and the temperature at the shock front increases, accordingly. Eventually this leads to strong x-ray self-emission, which heats the unshocked material in front of the shock and changes the assumption used in the Hugoniot equations that the unshocked material is cold. Recent experiments have measured the Hugoniot of CH plastic from 20 to 60 Mbar in a low-drive (300 kJ) NIF experiment,[5,6] while other experiments have

measured Hugoniot data of up to 800 Mbar in high-drive (1.1 MJ) NIF experiments.[7]

Many experiments[8–11] have measured the equation of state (EOS) of CH at low pressure, typically below 10 Mbar, even though Nova experiments[8] did reach up to 40 Mbar. Using quantum molecular dynamics (QMD), path integral Monte Carlo (PIMC), and other theoretical methods, many researchers have modeled[12–17] the EOS of plastics, such as CH, that are used as ablators in various experiments.

In this paper we look at the two sources of radiation heating for unshocked material and the effect this heating has on the interpretation of Hugoniot measurement. In addition to the x-ray self-emission at the shock front, we also examine the role of the target being preheated by the high-energy kilo-electron-volt x-rays from the hohlraum. We show that preheating is not an issue in low-drive NIF experiments that measure data from 40 to 130 Mbar, but that it can effectively heat targets to several electron-volt, placing the experiment on a slightly different Hugoniot for the high-drive Gbar experiments that measure 100s of Mbar. Our calculations estimate that the self-emission from the shock front limits the pressure that can be measured on the Hugoniot to about 400 Mbar, in the case of plastic, even when the experiment can measure data at up to 800 Mbar.

II. Gbar EXPERIMENTAL PLATFORM TO MEASURE HUGONIOT EOS DATA

The Gbar experimental platform is described in more detail in Refs. 4–7, but we give a brief overview of recent experiments that measure the EOS of poly(α-methylstyrene) C_9H_{10} (PAMS) plastic at pressures of 20–130 Mbar. A schematic of the experimental configuration is shown in Fig. 1(a). A more detailed description of the experiment can be found in Ref. 5. In these experiments, solid targets were compressed and heated in an indirect drive laser geometry using 176 laser beams, incident on an Au hohlraum. The targets consisted of solid CH spheres with a 970-μm radius, covered by a 185-μm-thick plastic ablator made of glow-discharge polymer (GDP) with a graded Ge (Z = 32) dopant. The Ge dopant served as both a marker layer in the experiment for radiography as well as a preheat shield to reduce preheating of the plastic target. The ablator consisted of four layers, as

shown in detail in Fig. 1. The second layer, which was 33 μm thick, was doped with 1.1% Ge by atomic fraction and served as the primary marker layer and preheat shield.

The experiments used a standard NIC scale 5.75 mm hohlraum (diameter = 5.75 mm, height = 9.42 mm) with a 0.03 mg/cc ^{4}He gas fill and 3.375 mm diameter laser entrance hole. The hohlraum was driven by 176, 351-nm laser beams. For the low-drive experiments[5,6] the pulse shape was a 4-ns long, nearly square pulse with a power of 78 TW. The total drive energy and power incident on the hohlraum walls was about ≅300 kJ for the low-drive experiments and 1.2 MJ for the high-drive experiments. These drive conditions result in a predicted peak hohlraum radiation temperature near 200 eV for the low-drive and 300 eV for the high drive experiment. In both cases the idea is to drive a single strong shock through the plastic target and measure a locus of Hugoniot points, as the shock propagates through the target.

III. RADIATION HYDRODYNAMIC SIMULATIONS

In this section we present radiation hydrodynamics design simulations to model and understand the EOS measurements using the Gbar platform and the sensitivity of the experiments to radiation preheating and self-emission from the shock front. To simplify the simulations, we changed the material slightly in the modeling to pure polystyrene, CH, at a density of 1.05 g/cc. These simulations were capsule-only simulations that used a frequency-dependent (FDS) radiation source that surrounded the capsule. This drive was derived from integrated hohlraum simulations using a detailed configuration accounting (DCA) atomic physics model.[18] The radiation drive was modified to account for the fact that 16 of the 192 drive beams were used to drive the backlighter for the streaked radiography. Radiation temperature as a function of time is plotted in Fig. 2, for the low-drive and high-drive experiments. The peak radiation temperature is predicted to be 191 and 286 eV for the low- and high-drive experiments, respectively. To model this in one dimension (1D) the simulations were conducted using the LASNEX radiation-hydrodynamic code.[19] The average-atom based tabular EOS table, LEOS 5400, was used for the CH sphere, and LEOS 5358 for the doped GDP ablator. The radiation transport was modeled using Sn multi-group radiation transport[20,21] with 110 radiation groups. To resolve
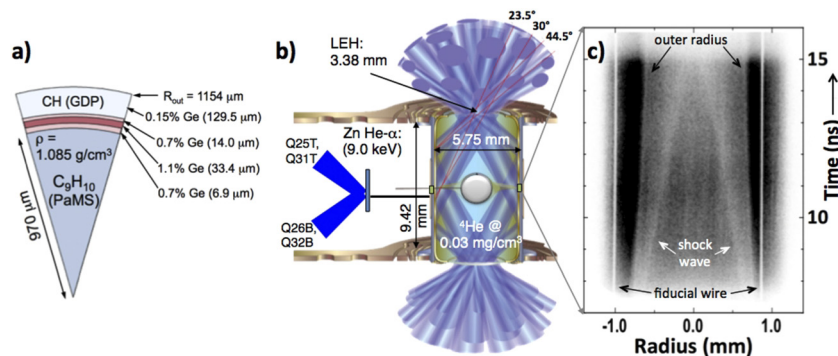

FIG. 1. (a) Schematic of the solid spherical CH target with Ge-doped GDP ablator used in the Gbar experiments. (b) Schematic of the experimental setup. Solid spherical target of CH is shock compressed using a hohlraum radiation drive, then backlit with ~9 keV Zn He-α x-rays to generate a time-resolved ("streaked") 1D image of the shock compression vs time. (c) Radiograph for the 9-keV x-ray backlighter vs time and radius, showing the shock wave converging to the central hot-spot. The vertical axis covers 8 ns and the horizontal axis covers a diameter of 0.2 cm. Details of the experiment are in Ref. 5.
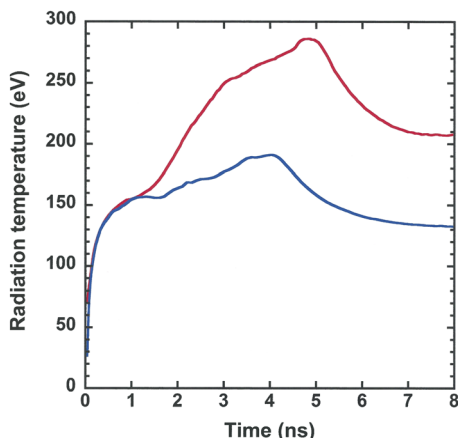
FIG. 2. Simulated radiation temperature vs time inside the radiation cavity (hohlraum) comparing the cases for high- (red) and low-drive (blue) Gbar experiments.

TABLE I. Pressure at shock front vs time and radius for low-drive Gbar simulation.

Time (ns)	Radius (μm)	Pressure (Mbar)
8.85	600	39
10.27	500	40
11.64	400	45
12.91	300	54
14.04	200	73
14.96	100	132

shock pressure vs position of the shock front. Table I shows how the pressure is initially near 39 Mbar when the shock is at a radius of 600 μm, slowly increasing to 73 Mb at a radius of 200 μm. Between radii of 200 and 100 μm, the pressure climbs more rapidly from 73 to 132 Mb, as the shock reaches 100 μm at t = 14.96 ns. Experimentally, it becomes difficult to measure the shock with adequate resolution below a radius of 100 μm, as the shock continues to accelerate inwards to the center. Figure 4 shows the pressure and density vs radius when the shock is at radii of 500 and 200 μm. At 500 μm, density and pressure both peak at the shock front, from where it is easy to extract the plasma parameters. As the radius decreases, the pressure increases slightly, while the density increases significantly behind the shock front, which is why the shock tracking routines must use derivatives of pressure to identify the shock front. This pileup of density behind the shock front is characteristic of the converging geometry.

Reference 6 gives a detailed description of how the Hugoniot data is extracted from the radiographic data in low-drive NIF experiments. The Rankine-Hugoniot relations are used to deduce the pressure, p_s, at the shock front from the measured shock velocity, u_s, and the density, ρ_s, at the shock front using $p_s = p_0 + \rho_0 \left[1 - \rho_0/\rho_s\right] (u_s)^2$, where ρ_0 is the unshocked density, and p_0 is the pressure in unshocked material.

Using the shock tracker, we can extract the Hugoniot data from the simulations. Figure 5 plots the pressure vs density from the simulation (red curve) and compares it with the Hugoniot (black

the shock front, the simulations used 0.25-μm zoning across the entire CH sphere.

For the low-drive experiment, the simulations predict that the ablation pressure at the boundary of the CH peaks at 41 Mbar at a time of 4.7 ns. The shock continues to travel inwards, slowly increasing as it reaches a radius of 600 μm around 8.85 ns. To understand how to extract Hugoniot data from the simulations we developed a shock-tracking routine that starts at the center of the calculation and looks for the first peak in entropy. This gives us the location of the rising edge of the incoming shock front. We then examine the pressure in adjacent zones and confirm that it does not change by more than 1% from zone to zone, defining this as the location of the shock. We have tried other methods, such as looking for the spatial derivative of the pressure to fall to 1%–3% of its peak value, and have obtained very similar results for the location of the shock front. In Fig. 3 we plot the
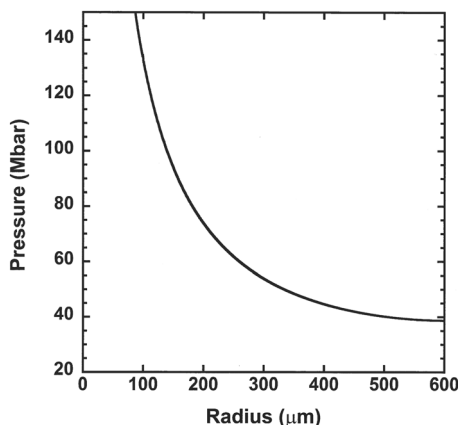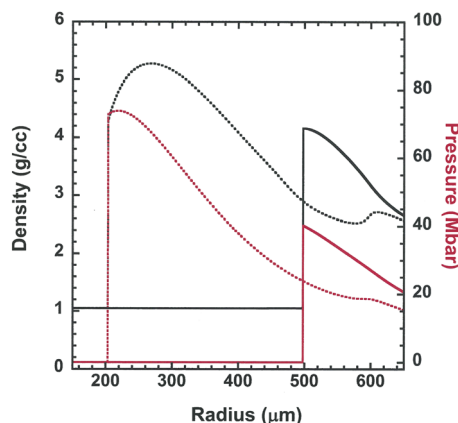

FIG. 3. Pressure at the shock front vs shock radius for low-drive Gbar simulations of a solid CH target. Pressure begins to increase steeply as the shock converges to radii of less than 200 μm.

FIG. 4. Snapshots of the simulated density (black) and pressure (red) vs the radius of the CH spherical target for the low-drive Gbar simulations at 10.3 and 14.0 ns. At an early time and large radius (solid), the pressure and density peak at the shock front. As the shock converges towards the center (dotted) there is a significant pileup in the density behind the shock.
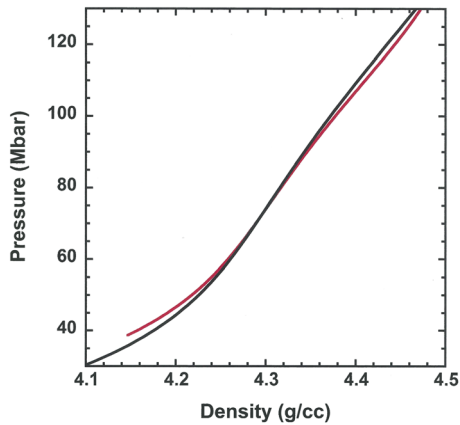
FIG. 5. The solid black line shows pressure vs density for the Hugoniot from the tabular EOS table LEOS 5400. The red curve represents the values of pressure and density extracted from the radiation-hydrodynamic simulations for the low-drive Gbar simulation of a solid CH target. There is excellent agreement, within 0.2%, over the pressure range of 50–130 Mbar.
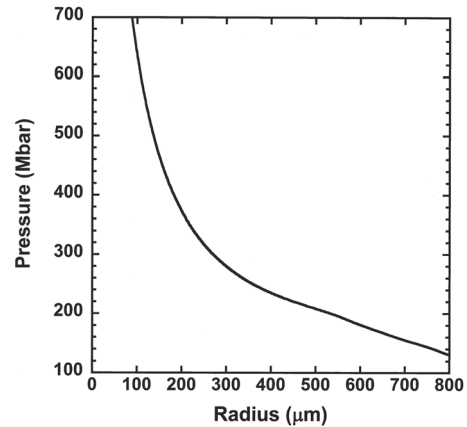

FIG. 6. Pressure at the shock front vs shock radius for the high-drive Gbar simulations of a solid CH target. Pressure begins to increase steeply as the shock converges to radii of less than 200 μm.

curve) from the LEOS 5400 table used in the calculation. There is excellent agreement between experiment and theory, within 0.2% over the entire pressure range of 50–130 Mbar, giving cause for great confidence that the experiment is a valid method for measuring Hugoniot data, even with a converging shock. Locally, the shock acts as a series of planar shocks, allowing one to extract a locus of Hugoniot data from a single experiment. We developed a method to smooth out the noise in the Hugoniot data extracted from the simulation by dividing the density vs pressure curve by the Hugoniot from the LEOS 5400 table, fitting the result to a fourth-order polynomial over the range of interest and then multiplying by the divisor of the previous ratio. To understand the effects of preheating in the low-drive experiment, we performed a calculation using an equivalent black-body radiation source that did not have the Au M-shell in the detailed frequency-dependent spectrum. If we use the fraction of radiation above 1.9 keV as a metric for M-shell radiation, our frequency-dependent source has 1.6% of the radiation above 1.9 keV, while the equivalent black-body source only has 0.2%. However, the Hugoniot data we extract using the temperature source looks virtually identical to that using the frequency-dependent source, indicating that pre-heating is not an issue in low-drive experiments. To quantify the effects of self-emission from the shock front, the simulation "zeroes out" the emission and absorption opacity for the unshocked material in front of the shock. This eliminates the effects of self-emission arising from the shock, heating any material in front of it. Again, the Hugoniot we extract from the simulation does not change, indicating that self-emission is not an issue in low-drive experiments that measure data up to a pressure of 130 Mb.

For a high-drive experiment, the simulations predict that the shock reaches the CH boundary at 3.15 ns, with an ablation pressure of 94 Mbar. The shock continues to travel inwards, beginning to slowly increase, as seen in Fig. 6 where we plot shock pressure vs shock-front position. Table II shows a shock pressure of 130 Mbar at a radius of 800 μm and time of 4.58 ns that slowly increases to 373 Mb, as the shock reaches a radius of 200 μm at 8.35 ns. Between 200 and 100 μm pressure starts to climb more rapidly from 373 to 638 Mb, as

the shock reaches 100 μm at t = 8.76 ns. As the shock continues to accelerate inwards to the center, the pressure doubles to over 1.1 Gbar in the next 160 ps, as the shock reaches a radius of 49 μm. Experimentally it becomes difficult to measure the shock with adequate resolution below a radius of 100 μm. It is also noteworthy that CH-plastic opacity at the 9-keV energy of the backlighter used in the experiments decreases to half of the cold opacity at a pressure of 400 Mb. As the Gbar EOS experiments reach higher pressures that enable one to see K-shell effects[7] on the Hugoniot, K-shell ionization causes the opacity values used in the radiographic unfold of the density to change significantly from the cold opacity values. Understanding how the opacity changes is vital to the analysis of the experimental data but is not used by our shock tracker in extracting the Hugoniot points in the simulations presented in this paper. The effects of changing opacity in the shocked regions will be discussed in a separate paper. The small temperature increase of up to 4 eV in front of the shock due to the preheat is not expected to affect the opacity of the 9-keV backlighter.

Figure 7 plots pressure vs density from the simulation (red solid) and compares it with the Hugoniot data from the LEOS 5400 table (black solid) used in the calculation. The simulation has a lower

TABLE II. Pressure at shock front vs time and radius for high-drive Gbar simulation.

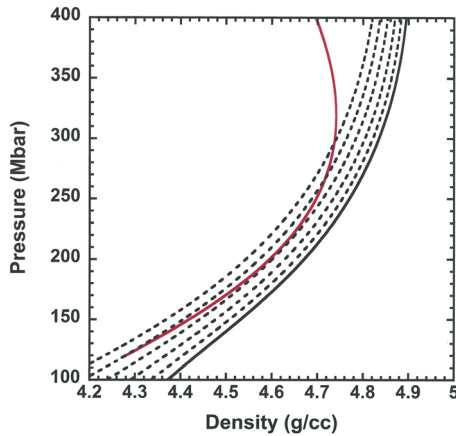| Time (ns)	Radius (μm)	Pressure (Mbar)
4.58	800	130
5.33	700	155
6.02	600	181
6.67	500	208
7.27	400	235
7.84	300	280
8.35	200	373
8.76	100	638
8.85	74	807
8.92	49	1122

FIG. 7. The solid black line shows pressure vs density for the Hugoniot from the tabular EOS table LEOS 5400. The dotted lines are the Hugoniot for LEOS 5400, with initial temperatures 1–5 eV, with 1 eV being closest to the solid curve. The red curve represents the values of pressure and density extracted from the radiation-hydrodynamic simulations for the high-drive Gbar simulation of a solid CH target. The simulation initially lies on a preheated Hugoniot between 3 and 4 eV.
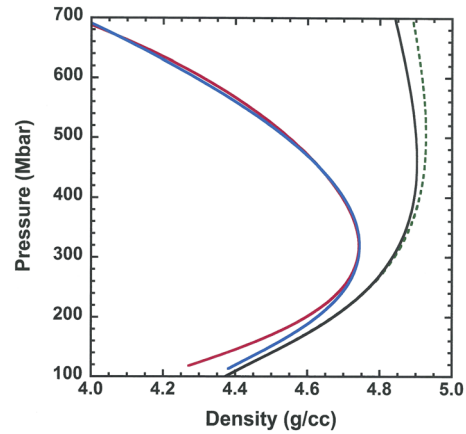

FIG. 8. The solid black line shows pressure vs density for the Hugoniot from tabular EOS table LEOS 5400. The red curve represents the values of pressure and density extracted from the radiation-hydrodynamic simulations using the full FDS source for the high-drive Gbar simulation of a solid CH target. The blue curve uses an equivalent black-body source to drive the CH target, while the green dotted curve uses the full FDS source but zeroes out the opacity in front of the shock to eliminate the effects of preheating and radiative heating from the shock on unshocked material.

density, even at the lowest pressures near 100 Mb. To understand this, we also plotted a series of Hugoniots (black dotted) with initial temperatures varying from 1 to 5 eV, with the 1-eV curve being closest to the nominal Hugoniot. The simulated Hugoniot begins at an effective temperature of 3–4 eV due to preheat from the hohlraum source. After the laser drive turns off, the preheat starts to decrease and, initially, the simulation moves closer to the baseline Hugoniot. As the pressure climbs above 300 Mb, the density begins to bend to lower densities due to self-emission from the shock front heating unshocked material.

To understand the effects of preheating in high-drive experiments we performed a calculation using an equivalent black-body radiation source that had no Au M-shell in the detailed frequency-dependent spectrum. Using the fraction of radiation above 1.9 keV as a metric for M-shell radiation, our frequency-dependent source has 10.4% of radiation above 1.9 keV, while the equivalent black-body source only has 4.9%. While this reduces preheating, it does not eliminate it, as indicated by the blue solid curve in Fig. 8, which shows the simulated Hugoniot using this temperature source. The effective temperature is now estimated to be between 1 and 2 eV.

To eliminate both the preheating from the hohlraum and the self-emission from the shock front, we ran a simulation, zeroing out the emission and absorption opacity for the unshocked material in front of the shock, as shown by the green dotted curve in Fig. 8. We first identified the shock front and then zeroed out the opacity only in the unshocked material at each time step in the simulation. By zeroing out the opacity, the unshocked material does not absorb radiation and is not heated by any of the x-rays emitted in the hot plasma at and behind the shock front. In this case, the simulation closely follows the Hugoniot curve, up to pressures of 400 Mb and above; it does slightly drift to higher density, but even at 700 Mb, the density is only 1% above the Hugoniot value. That we can remove the effects of preheating and self-emission in the simulations gives us confidence in our ability to model and quantify these effects.

Based on these calculations, for high-drive Gbar experiments using a PAMS target, we would want to limit our Hugoniot data to a pressure of about 400 Mb, even though the experimental data would attain 650 Mb at a minimum radius of 100 μm. These are estimates, and other models give similar results with slightly different estimates of 450 Mbar for the maximum pressure to use for extracting the Hugoniot data.

To illustrate preheating effects, we examine temperature and density lineouts at 5.0 ns, the time of the peak in the laser drive and preheating in the high-drive simulation. The shock pressure is 145 Mbar. Figure 9 plots the electron temperature vs radius when the
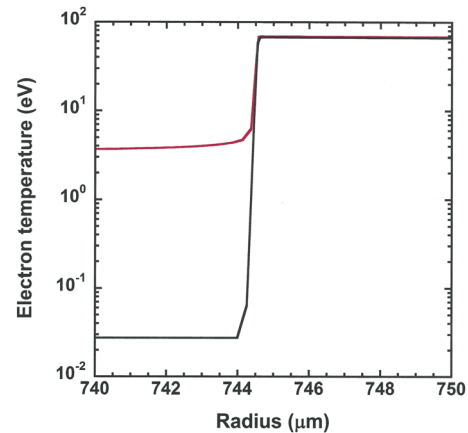

FIG. 9. Snapshots of the simulated electron temperature vs the radius of the CH spherical target for the high-drive Gbar simulations, when the shock reaches a 744-μm radius at time 5.0 ns. The red curve is the baseline simulation using the full FDS source, while the black curve is the same simulation with the opacity zeroed out in front of the shock to eliminate radiation heating effects. Radiation heating from the preheating heats unshocked material to temperatures of about 4 eV in front of the shock.
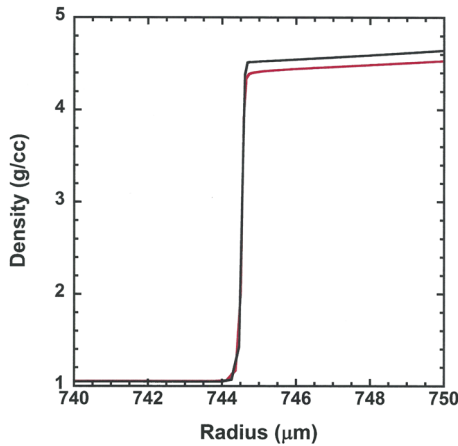
FIG. 10. Snapshots of the simulated density vs the radius of the CH spherical target for the high-drive Gbar simulations when the shock reaches a 744-μm radius at time 5.0 ns. The red curve is the baseline simulation using the full FDS source, while the black curve is the same simulation with the opacity zeroed out in front of the shock to eliminate radiation heating effects. The density is about 2% lower in the preheated case.

FIG. 12. Snapshots of the simulated electron temperature vs the radius of the CH spherical target for the high-drive Gbar simulations when the shock reaches an 89-μm radius at time 8.8 ns. The red curve is the baseline simulation using the full FDS source, while the black curve is the same simulation with the opacity zeroed out in front of the shock to eliminate radiation heating effects. Radiation heating from the shock heats the unshocked material to temperatures exceeding 50 eV in front of the shock.

shock is at 744 μm for the nominal simulations (red solid) that include the effects of preheating, compared with (black solid) when we zero out the opacity in front of the shock to eliminate radiation effects on the Hugoniot. The temperature in front of the shock is about 4 eV when preheating is included, which is consistent with the Hugoniot values we extract from the simulation in Fig. 7. To see how preheating affects density, Fig. 10 plots density vs radius for these two cases with and without the effects of preheating. The density is 2% lower for the red curve that includes the effects of preheating.

To better understand the challenges in this type of experiment and why the simulations drift to low density from the self-emission, we examine lineouts of the temperature, pressure, and density at a time of 8.8 ns in the high-drive simulation. Figure 11 shows pressure
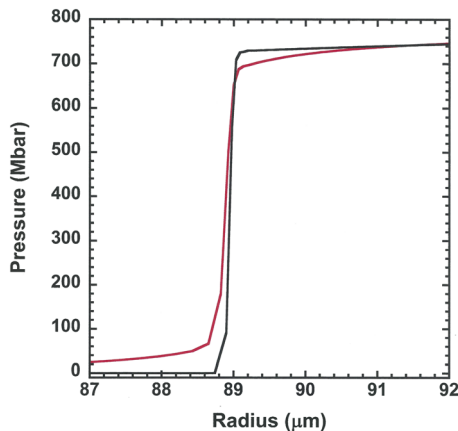
vs radius near the shock front when the shock is at 89 μm for the nominal simulations (red solid) that include the effects of preheating and self-emission, compared with (black solid) when we zero out the opacity in front of the shock to eliminate radiation effects on the Hugoniot. The pressures are similar, within 5%, while the electron temperature, shown in Fig. 12 rises significantly near the shock front and falls off rather slowly in front of the shock when the full simulation with radiation is included. The temperature exceeds 50 eV in the unshocked material. Figure 13 plots density vs radius, and self-

FIG. 11. Snapshot of the simulated pressure vs the radius of the CH spherical target for the high-drive Gbar simulations when the shock reaches an 89-μm radius at time 8.8 ns. The red curve is the baseline simulation using the full FDS source, while the black curve is the same simulation with the opacity zeroed out in front of the shock to eliminate radiation heating effects.
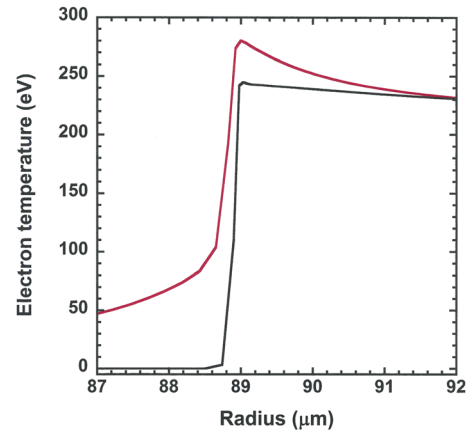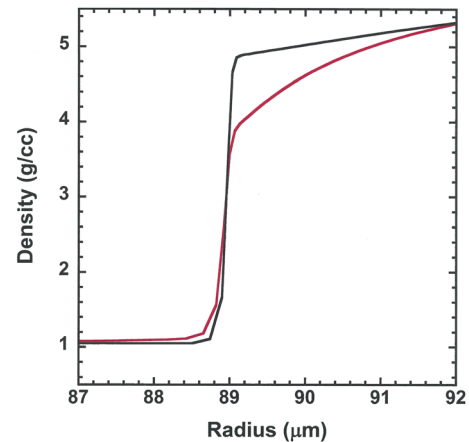

FIG. 13. Snapshots of the simulated density vs the radius of the CH spherical target for the high-drive Gbar simulations when the shock reaches an 89-μm radius at time 8.8 ns. The red curve is the baseline simulation using the full FDS source, while the black curve is the same simulation with the opacity zeroed out in front of the shock to eliminate radiation heating effects. The density has dropped significantly at the shock front due to radiative heating.

emission rounds off the sharp jump in density and makes the density at the shock front about 18% lower than the case without the effects of preheating, even though the overall shapes of the density curves are very similar behind the shock. Self-emission causes very substantial heating of unshocked material, driving the experiment off the Hugoniot curve. In future experiments, it would be interesting to try to directly measure the effects of radiative heating on the Hugoniot.

IV. CONCLUSIONS

For low-drive Gbar EOS experiments using CH targets, simulations show that the shock front lies nicely on the Hugoniot in the pressure range of 40–130 Mbar, and that the effects of radiation preheating and self-emission from the shock front do not have any significant effect on Hugoniot measurements. Simulations give cause for confidence that the shock front for the converging geometry Gbar EOS experiments is indeed on the Hugoniot. The situation is quite different for high-drive Gbar simulations. In these cases high-energy x-rays from the hohlraum preheat unshocked material and cause the experiment to lie on a preheated Hugoniot, with temperatures near 3–4 eV at early times in the shock convergence. As the shock converges towards the center, the self-emission from the shock front begins to heat unshocked material even more and drives the experiment further off the Hugoniot. Using 5% uncertainty in the experimental measurement of density as a benchmark, we estimate that the effects of self-emission begin to become significant above pressures of 400 Mb.

REFERENCES

[1]L. Stixrude, Phys. Rev. Lett. **108**, 055505 (2012).

[2]S. Seager et al., Astrophys. J. **669**, 1279 (2007).

[3]V. E. Fortov, Extreme States of Matter on Earth and in the Cosmos (Springer-Verlag, Heidelberg, 2011), p. 224.

[4]A. L. Kritcher, T. Döppner, D. Swift, J. Hawreliak, G. Collins, J. Nilsen, B. Bachmann, E. Dewald, D. Strozzi, S. Felker, O. L. Landen, O. Jones, C. Thomas, J. Hammer, C. Keane, H. J. Lee, S. H. Glenzer, S. Rothman, D. Chapman, D. Kraus, P. Neumayer, and R. W. Falcone, "Probing matter at Gbar pressures at the NIF," High Energy Density Phys. **10**, 27–34 (2014).

[5]T. Döppner, D. C. Swift, A. L. Kritcher, B. Bachmann, G. W. Collins, D. A. Chapman, J. Hawreliak, D. Kraus, J. Nilsen, S. Rothman, L. X. Benedict, E. Dewald, D. E. Fratanduono, J. A. Gaffney, S. H. Glenzer, S. Hamel, O. L. Landen, H. J. Lee, S. LePape, T. Ma, M. J. MacDonald, A. MacPhee, D. Milathianaki, M. Millot, P. Neumayer, P. A. Sterne, R. Tommasini, and R. W. Falcone, "Absolute equation-of-state measurements for polystyrene from 25 to 60 Mbar using a spherically converging shock wave," Phys. Rev. Lett. **121**, 025001 (2018).

[6]D. C. Swift, A. L. Kritcher, J. A. Hawreliak, A. Lazicki, A. MacPhee, B. Bachmann, T. Döppner, J. Nilsen, G. W. Collins, S. Glenzer, S. D. Rothman, D. Kraus, and R. W. Falcone, "Absolute Hugoniot measurements from a spherically-convergent shock using x-ray radiography," Rev. Sci. Instrum. **89**, 053505 (2018).

[7]High drive Gbar experiments are in the process of being analyzed and are not yet published

[8]R. Cauble, L. B. Da Silva, T. S. Perry, D. R. Bach, K. S. Budil, P. Celliers, G. W. Collins, A. Ng, T. W. Barbee, Jr., B. A. Hammel, N. C. Holmes, J. D. Kilkenny, R. J. Wallace, G. Chiu, and N. C. Woolsey, "Absolute measurements of the equation of state of low-Z materials in the multi-Mbar regime using laser-driven shocks," Phys. Plasmas **4**, 1857–1861 (1997).

[9]M. Koenig, F. Philippe, A. Benuzzi-Mounaix, D. Batani, M. Tomasino, E. Henry, and T. Hall, "Optical properties of highly compressed polystyrene using laser-driven shockwaves," Phys. Plasmas **10**, 3026–3029 (2003).

[10]N. Ozaki et al., "Shock Hugoniot and temperature data for polystyrene obtained with quartz standard," Phys. Plasmas **16**, 062702 (2009).

[11]M. A. Barrios, D. G. Hicks, T. R. Boehly, D. E. Fratanduono, J. H. Eggert, P. M. Celliers, G. W. Collins, and D. D. Meyerhofer, "High-precision measurements of the equation of state of hydrocarbons at 1–10 Mbar using laser-driven shock waves," Phys. Plasmas **17**, 056307 (2010).

[12]C. Wang, X.-T. He, and P. Zhang, "Thermophysical properties for shock compressed polystyrene," Phys. Plasmas **18**, 082707 (2011).

[13]S. Hamel et al., "Equation of state of $CH_{1.36}$: First-principles molecular dynamics simulations and shock-and-release wave speed measurements," Phys. Rev. B **86**, 094113 (2012).

[14]S. X. Hu, T. R. Boehly, and L. A. Collins, "Properties of warm dense polystyrene plasmas along the principal Hugoniot," Phys. Rev. E **89**, 063104 (2014).

[15]S. X. Hu, L. A. Collins, V. N. Goncharov, J. D. Kress, R. L. McCrory, and S. Skupsky, "First-principles equation of state of polystyrene and its effect on inertial confinement fusion implosions," Phys. Rev. E **92**, 043104 (2015).

[16]P. Colin-Lalu, V. Recoules, G. Salin, T. Plisson, E. Brambrink, T. Vinci, R. Bolis, and G. Huser, "Dissociation along the principal Hugoniot of the laser megajoule ablator material," Phys. Rev. E **94**, 023204 (2016).

[17]S. Zhang, B. Militzer, L. X. Benedict, F. Soubiran, P. A. Sterne, and K. P. Driver, "Path integral Monte Carlo simulations of dense carbon-hydrogen plasmas," J. Chem. Phys. **148**, 102318 (2018).

[18]M. Rosen et al., High Energy Density Phys. **7**, 180–190 (2011).

[19]G. B. Zimmerman and W. L. Kruer, Comments Plasma Phys. Controlled Fusion **2**, 51–61 (1975).

[20]M. K. Nemanic and P. Nowak, "Radiation transport calculations on unstructured grids using a spatially decomposed and threaded algorithm," in Mathematics and Computation, Reactor Physics and Environmental Analysis in Nuclear Applications, Madrid (ES), April 1999.

[21]P. G. Maginot, P. F. Nowak, and M. L. Adams, "A review of the upstream corner balance spatial discretization," in International Conference on Mathematics and Computational Methods, Applied to Nuclear Science and Engineering, Jeju, Korea, April 2017.